



LAWRENCE
LIVERMORE
NATIONAL
LABORATORY

Neutron Crosstalk between Liquid Scintillators

J. M. Verbeke, M. K. Prasad, N. J. Snyderman

January 28, 2015

Nuclear Instruments and Methods in Physics Research
Section A: Accelerators, Spectrometers, Detectors and
Associated Equipment

Disclaimer

This document was prepared as an account of work sponsored by an agency of the United States government. Neither the United States government nor Lawrence Livermore National Security, LLC, nor any of their employees makes any warranty, expressed or implied, or assumes any legal liability or responsibility for the accuracy, completeness, or usefulness of any information, apparatus, product, or process disclosed, or represents that its use would not infringe privately owned rights. Reference herein to any specific commercial product, process, or service by trade name, trademark, manufacturer, or otherwise does not necessarily constitute or imply its endorsement, recommendation, or favoring by the United States government or Lawrence Livermore National Security, LLC. The views and opinions of authors expressed herein do not necessarily state or reflect those of the United States government or Lawrence Livermore National Security, LLC, and shall not be used for advertising or product endorsement purposes.

Neutron crosstalk between liquid scintillators

J.M. Verbeke*, M.K. Prasad*, N.J. Snyderman*

Lawrence Livermore National Laboratory, P.O. Box 808, Livermore, CA 94551, United States

Abstract

A method is proposed to quantify the fractions of neutrons scattering between liquid scintillators. Using a spontaneous fission source, this method can be utilized to quickly characterize an array of liquid scintillators in terms of crosstalk. The point model theory due to Feynman is corrected to account for these multiple scatterings. Using spectral information measured by the liquid scintillators, fractions of multiple scattering can be estimated, and mass reconstruction of fissile materials under investigation can be improved. Monte Carlo simulations of mono-energetic neutron sources were performed to estimate neutron crosstalk. A californium source in an array of liquid scintillators was modeled to illustrate the improvement of the mass reconstruction.

Keywords: liquid scintillators, crosstalk, multiple scattering, neutron multiplicity, neutron correlation, fissile materials

1. Introduction

The purpose of this work is to quantify the fractions of fast neutrons scattering between adjacent liquid scintillators, a phenomenon known as neutron crosstalk. We propose a new method to quantify them. While this paper will focus on theoretical development to model neutron crosstalk, and show simulation results, the strength of this new method lies in that it can be used to determine neutron crosstalk experimentally using fissile materials as neutron sources. This will enable experimentalists to quickly characterize their array of liquid scintillators in terms of multiple scattering fractions/neutron crosstalk, the same way as instruments are calibrated in energy, and detectors are synchronized in time, prior to taking data. The authors are currently working on a second paper, where an array of liquid scintillators is thus characterized experimentally. Preliminary results are available in Ref. [1].

It is well known [2, 3, 4, 5] that masses of nuclear materials undergoing fissions can be determined using ^3He tubes counting thermal neutrons. For general neutron multiplicity counting (NMC) applications, the theory usually assumes that neutrons can only be counted once. This assumption is correct for ^3He tubes, where neutrons are captured when counted. However, for liquid scintillators, a neutron can scatter and deposit enough energy in multiple liquid scintillators to record multiple counts. The measured count rate and the two- and three-neutron correlations will thus be adversely increased. NMC applications are very sensitive to two-, three- and higher order correlations. With fast neutrons registering multiple correlated counts, the standard Feynman

28 moment method [2, 3, 4, 5] will fail. In this paper, new expressions of the Feynman
29 correlated moments are proposed to account for multiple scattering.

30 A summary of this paper is as follows. In Sec. 2, we derive new expressions for the
31 Feynman correlated moments to account for individual neutrons scattering and record-
32 ing multiple counts in detectors.

33 Since neutron crosstalk depends on the energy of the neutrons incident on the detec-
34 tors, it must be characterized as a function of this incident neutron energy. In Sec. 3, we
35 simulate the liquid scintillator response to different mono-energetic neutron sources,
36 from which we infer the spectrum of incident neutrons (Sec. 4), and in turn the expected
37 multiple scattering fractions (Sec. 5). The inferred neutron source energy spectrum re-
38 veals information about the source under investigation. This spectral information has
39 been successfully used experimentally in Ref. [6].

40 In the last part of this paper, Sec. 6, we simulate a ^{252}Cf source in an array of
41 liquid scintillators. We will show that the multiple scattering fractions inferred from
42 the spectrum of deposited energies can be used to apply corrections to the masses of
43 fissile materials undergoing fission.

44 A list of symbols used throughout the text is available in the appending nomencla-
45 ture.

46 2. Theory

47 When a multiplying object is placed in the center of a liquid scintillator array such
48 as the one shown in Fig. 1, one can experimentally measure the times of arrival of the
neutrons in each of the liquid scintillators. Randomly splitting the sequence of time

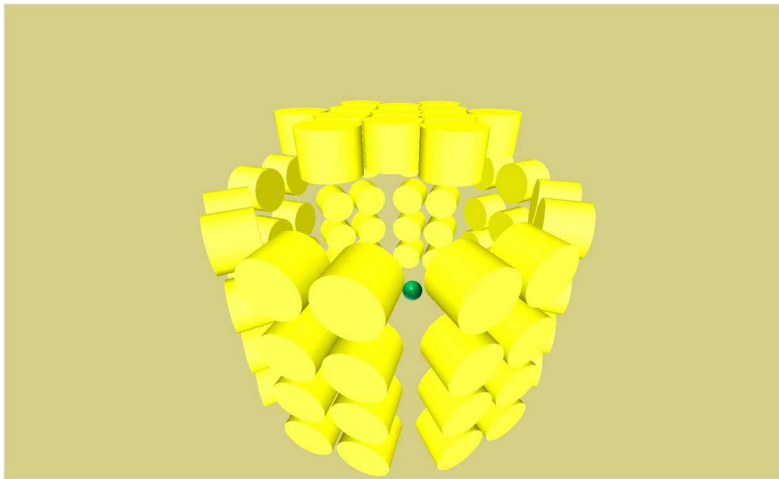


Figure 1: Multiplying object in the middle of a 77 liquid scintillator array.

49 tags into N segments of duration T ,¹ one can count how many neutrons arrive in the

¹ T is of the order of nanoseconds to hundreds of microseconds.

51 first segment, how many in the second segment, in the third one, etc. and build the
 52 distribution $B_n(T)$ of the number of neutrons n arriving in the segments of duration
 53 T . By repeating this procedure for segments of different durations T , multiple count
 54 distributions $B_n(T)$ can be obtained.

These count distributions $B_n(T)$ can be used to determine the intensity F_s of the spontaneous fission sources in the object, the efficiency ε of the liquid scintillator array and the multiplication M of the multiplying object. This will be shown by way of the following three equations. Defining $b_n(T)$ as the probability distribution of the count distribution $B_n(T)$,² one can show theoretically that the first moment of the probability distribution $b_n(T)$ can be written as [3, 4]

$$\bar{C}(T) = \varepsilon q M \bar{v}_{\text{sp}} F_s (1 + A) T \quad (1)$$

where F_s is the intensity of the spontaneous fission source (in units of spontaneous fissions per second), and A is the α -ratio³, i.e. the ratio of neutrons emitted by sources emitting single neutrons to neutrons emitted by sources emitting multiple neutrons simultaneously. In this equation, let us recall that the multiplication M is defined as

$$M = \frac{1}{1 - p\bar{v}} \quad (2)$$

where p is the probability that a neutron will fission a nucleus, and $q = 1 - p$ is the probability that a neutron does not induce fission. qM is usually referred to as the escape multiplication⁴ and is given by

$$qM = M - (M - 1)/\bar{v} \quad (3)$$

The symbols \bar{v} and \bar{v}_{sp} are the average numbers of neutrons emitted per induced and spontaneous fissions, respectively. \bar{v} can be calculated as

$$\bar{v} = \sum_{n=1}^8 n C_n \quad (4)$$

55 where C_n is the probability of emitting n neutrons per induced fission. The upper
 56 limit of 8 on the summation sign is the largest number of neutrons that known isotopes
 57 produce per fission. The probability distribution C depends on the energy of the neutron
 58 inducing fission. To obtain \bar{v}_{sp} , the multiplicity distribution C is replaced by C^{sp} .

For time-gated fast neutron counting, the Feynman correlated moment Y_{2F} , which is the excess over unity of the variance to mean ratio of $b_n(T)$, or physically speaking the correlated pairs relative to the counts, is a generalization of Eq. (132) in Ref. [4] divided by $\bar{C}(T)$ (Eq. (1) above),

$$Y_{2F}(T) = \varepsilon q M \left[\frac{D_{2s}}{1 + A} + (M - 1) D_2 \right] \left(1 - \frac{1 - e^{-\alpha T}}{\alpha T} \right) \quad (5)$$

²This is equivalent to normalizing $B_n(T)$ by the number of segments of duration T : $b_n(T) = B_n(T)/N$.

³We use A in lieu of α for the alpha-ratio, we reserve the greek letter α for the inverse fission chain evolution time scale.

⁴Or leakage multiplication.

where α is a time constant related to the transport of the neutrons in both the measured object and the detection system. D_{2s} , D_2 are combinatorial moments of spontaneous and induced fission multiplicity distributions. They depend on nuclear data, and are in general given by

$$D_n = \frac{\sum_{i=n}^8 \binom{i}{n} C_i}{\bar{v}}. \quad (6)$$

59 For spontaneous fission nuclear data, $D_{n \text{ sp}}$ is calculated similarly, replacing the multi-
60 plicity distribution C by the multiplicity distribution C^{sp} .

Y_{3F} , which is the skewness to mean ratio of $b_n(T)$, or physically speaking the correlated triples relative to the counts, is a generalization of Eq. (133) in Ref. [4] divided by $\bar{C}(T)$ (Eq. (1) above),

$$Y_{3F} = (\varepsilon q M)^2 \left[\left[\frac{D_{3s}}{1+A} + (M-1)D_3 \right] \left(1 - \frac{3 - 4e^{-\alpha T} + e^{-2\alpha T}}{2\alpha T} \right) + \left[2(M-1) \frac{D_{2s}D_2}{1+A} + 2(M-1)^2 D_2^2 \right] \left(1 - \frac{2 - (2 + \alpha T)e^{-\alpha T}}{\alpha T} \right) \right] \quad (7)$$

It is important to note that for uncorrelated random Poisson sources, Y_{2F} and Y_{3F} are identically zero and therefore provide a quantitative measure of correlation. We define R_{3F_1} and R_{3F_2} as

$$R_{3F_1} = (\varepsilon q M)^2 \left[\frac{D_{3s}}{1+A} + (M-1)D_3 \right] \quad (8)$$

$$R_{3F_2} = (\varepsilon q M)^2 \left[2(M-1) \frac{D_{2s}D_2}{1+A} + 2(M-1)^2 D_2^2 \right] \quad (9)$$

so that Eq. (7) can be rewritten as

$$Y_{3F} = R_{3F_1} \left(1 - \frac{3 - 4e^{-\alpha T} + e^{-2\alpha T}}{2\alpha T} \right) + R_{3F_2} \left(1 - \frac{2 - (2 + \alpha T)e^{-\alpha T}}{\alpha T} \right) \quad (10)$$

61 Fig. 2 shows an example of $Y_{2F}(T)$ and $Y_{3F}(T)$. The time constant α^{-1} is 6 ns and the
62 asymptotical value of $Y_{2F}(T)$ is 0.1174.

The slope of Eq. (1) and the asymptotes of Eqs. (5) and (7) for large time gate durations T can be written as

$$\begin{cases} R_1 = \varepsilon q M \bar{v}_{\text{sp}} F_s (1+A) \\ R_{2F} = \varepsilon q M \left[\frac{D_{2s}}{1+A} + (M-1)D_2 \right] \\ R_{3F} = (\varepsilon q M)^2 \left[\frac{D_{3s}}{1+A} + (M-1)D_3 + 2(M-1) \frac{D_{2s}D_2}{1+A} + 2(M-1)^2 D_2^2 \right] \end{cases} \quad (11)$$

This system of 3 equations has 4 unknowns ε , M , F_s and A . In the absence of (α, n) sources which emit single neutrons at a time, the ratio A is equal to zero. In this case, the system of equations (11) reduces to

$$\begin{cases} R_1 = \varepsilon q M \bar{v}_{\text{sp}} F_s \\ R_{2F} = \varepsilon q M [D_{2s} + (M-1)D_2] \\ R_{3F} = (\varepsilon q M)^2 [D_{3s} + (M-1)D_3 + 2(M-1)D_{2s}D_2 + 2(M-1)^2 D_2^2] \end{cases} \quad (12)$$

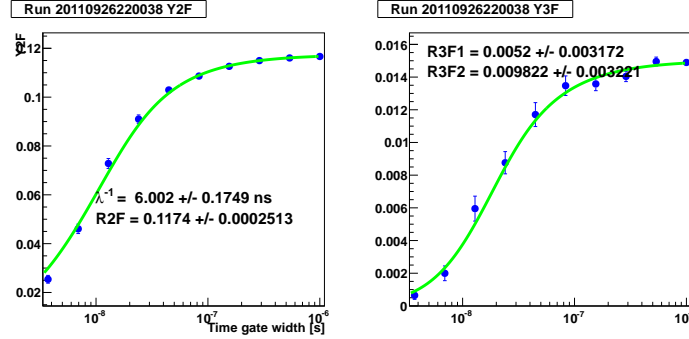


Figure 2: Examples of $Y_{2F}(T)$ and $Y_{3F}(T)$. λ^{-1} refers to α^{-1} .

63 2.1. Detector corrections

These equations rely on the assumption that each neutron in the system can be detected only once. This is certainly true for a detection system based on ^3He tubes, because ^3He captures the neutron and the neutron disappears from the system. It is different in an array of liquid scintillators, because neutrons in such a system deposit energy in scintillators by scattering with the atoms, and are not absorbed in these elastic and inelastic scattering collisions. They keep traveling, and if they still have enough energy, they can potentially deposit this energy in adjacent or even remote scintillators. If a neutron scatters multiple times between liquid scintillators, Eqs. (1), (5) and (7) no longer hold. They can however be replaced by ones that account for the multiple scattering of neutrons (the derivation of these equations is in [Appendix A](#) and assumes no more than triply counted neutrons.⁵):

$$\begin{cases} \bar{C}(T) = \left[(1 - f_2 - f_3) + \binom{2}{1} f_2 + \binom{3}{1} f_3 \right] R_1^* T \\ Y_{2F}(T) = \frac{f_2 + 3f_3}{1 + f_2 + 2f_3} + (1 + f_2 + 2f_3) \varepsilon q M \left[\frac{D_{2s}}{1+A} + (M-1)D_2 \right] \left(1 - \frac{1 - e^{-\alpha T}}{\alpha T} \right) \\ Y_{3F}(T) = \frac{f_3}{1 + f_2 + 2f_3} + 2(f_2 + 3f_3) \varepsilon q M \left[\frac{D_{2s}}{1+A} + (M-1)D_2 \right] \left(1 - \frac{1 - e^{-\alpha T}}{\alpha T} \right) \\ \quad + (1 + f_2 + 2f_3)^2 (\varepsilon q M)^2 \\ \quad \left[\left[\frac{D_{3s}}{1+A} + (M-1)D_3 \right] \left(1 - \frac{3 - 4e^{-\alpha T} + e^{-2\alpha T}}{2\alpha T} \right) + \left[2(M-1) \frac{D_{2s}D_2}{1+A} + 2(M-1)^2 D_2^2 \right] \left[1 - \frac{2 - (2 + \alpha T) e^{-\alpha T}}{\alpha T} \right] \right] \end{cases} \quad (13)$$

R_1^* is the hypothetical count rate which one would measure if individual neutrons could not be counted multiple times, as opposed to the measured count rate R_1 which includes 2 counts instead of 1 for each double scatter and 3 counts instead of 1 for each triple

⁵While the derivations in [Appendix A](#) could easily be generalized to neutrons scattering any number of times, equations (13) assume that individual neutrons do not register counts in more than 3 liquid scintillators on physical grounds laid out below.

scatter.⁶ f_2 is the ratio of the doubles rate to R_1^* , f_3 is the ratio of the triples rate to R_1^* . For multiple scattering, R_1 is defined as

$$R_1 = (1 + f_2 + 2f_3) R_1^* \quad (14)$$

64 The first equation for $\bar{C}(T)$ in the system of equations (13) is the sum of three terms,
 65 all factors of $R_1^* T$. The first term is the fraction of single neutrons that are counted
 66 as such, the second term is $\binom{2}{1}$ times the fraction of single neutrons that are counted
 67 twice, the third term is $\binom{3}{1}$ times the fraction of single neutrons that are counted thrice.
 68 As a matter of consistency, let us assume the case where single neutrons always double
 69 scatter but never triple scatter. In this case f_2 is 1 and f_3 is 0, so that the number of
 70 counted neutrons within a time gate T is $\bar{C}(T) = \binom{2}{1} R_1^* T$, which is twice the number
 71 of real single neutrons. The same could be said for the case of neutrons always triple
 72 scattering.

73 Let us examine the assumption that neutrons cannot register counts in more than
 74 3 liquid scintillators. For a single neutron to deposit more than 1.2 MeV — which
 75 is approximately the liquid scintillator threshold energy for detecting fast neutrons —
 76 in 4 different liquid scintillators, it would theoretically only need to have an initial
 77 energy of 4.8 MeV. In reality however, a neutron would need to have a much higher
 78 energy to record counts in 4 different liquid scintillators with a reasonable probability.
 79 In Fig. 3, we show that the probability of a neutron registering 4 counts in 4 different
 liquid scintillators is negligible for any neutron below 10 MeV. Since the purpose here

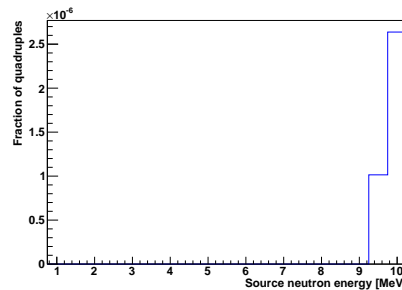


Figure 3: Fraction of detected neutrons registering four counts in the liquid scintillators, as a function of the source neutron energies.

80 is to study fast neutrons with energies similar to the ones found in fission spectra, we
 81 can safely neglect any multiple scattering greater than 3.

82 Once we know f_2 and f_3 , and if we assume that A is zero, the system of equa-
 83 tions (13) corrected for multiple scattering can be solved for the three system param-
 84 eters: the intensity F_s of the spontaneous fission source, the multiplication M of the ob-
 85 ject, and the efficiency ϵ of the detection system. Our goal is to determine whether the
 86

⁶To illustrate R_1^* , if a neutron was to multiple scatter between different liquid scintillators, this neutron would contribute only a single count towards the hypothetical R_1^* , in lieu of contributing multiple counts.

87 multiple scattering fractions f_2 and f_3 can be determined from measuring the spectrum
88 of energies deposited by the fast neutrons from a single measurement, that is without
89 any prior measurement. If this were the case, we could easily use these fractions to
90 apply a correction to the system parameters.

91 3. Neutron energy sensitivity study

92 In this section, we are studying the detector response to isotropic and mono-energetic
93 neutron sources. The goal is to determine whether spectral information measured ex-
94 perimentally by the detectors can be used to infer the energy distribution of the neutrons
95 entering the detectors⁷, and in turn to infer the multiple scattering values f_2 and f_3 . In
96 Secs. 4 and 5, we will infer the values of f_2 and f_3 from this spectral information.

97 For this study, we considered the liquid scintillator array shown in Fig. 1. We
98 placed a point neutron source in the middle of the array of liquid scintillators depicted
99 in Fig. 1. Neutrons are emitted isotropically and one at a time from that point source.
100 For 19 different mono-energetic neutron beams ranging from 1 MeV to 10 MeV in
101 increments of 0.5 MeV, we use the Monte Carlo radiation transport code MCNPX [7, 8]
102 to transport the neutrons from the point source in the middle of the array through the
103 geometry consisting of the array of liquid scintillators. The black curve in Fig. 4 shows
104 the energies of the neutrons entering the liquid scintillators, that had an initial kinetic
105 energy of 10 MeV. These were calculated by MCNPX using a flux tally. The other colors
correspond to neutrons with different initial kinetic energies. One notices that most

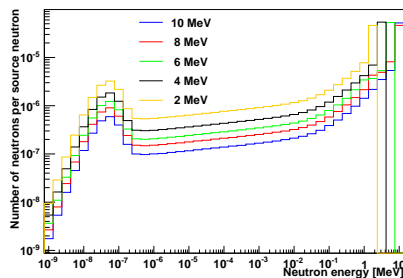


Figure 4: Energy distributions of fast neutrons entering the liquid scintillators as tallied by a MCNPX flux tally. The different colors refer to the different initial neutron energies. (For interpretation of the references to color in this figure caption, the reader is referred to the web version of this paper.)

106 neutrons enter the liquid scintillators with their full initial energy, but there is also
107 a second relatively strong peak from neutrons which have been thermalized by the
108 hydrogen in the liquid scintillators themselves.

109 In liquid scintillators, the reaction used for neutron detection is inelastic scatter-
110 ing of neutrons primarily on hydrogen, producing a recoil proton from which scin-
111 tillation light is emitted. A decade ago, LLNL developed a customized version [9]
112

⁷Or the energy distribution of the neutron source itself if it is not shielded.

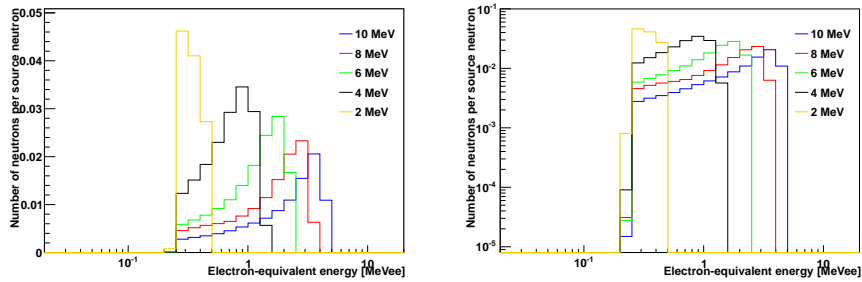


Figure 5: Electron-equivalent energy distribution measured by the liquid scintillators as predicted by MCNPX. The different colors refer to the different initial neutron energies. (For interpretation of the references to color in this figure caption, the reader is referred to the web version of this paper.)

113 of MCNPX which writes out detection events to an output file in “list-mode”. Using a
 114 quench function, each individual proton recoil energy in this file is converted to a cor-
 115 responding electron-equivalent energy E_d , in terms of scintillation light output. This
 116 electron-equivalent energy is what liquid scintillators effectively measure and has units
 117 of MeVee. The measured spectrum of energies deposited by fast neutrons is shown in
 118 Fig. 5, where multiple scattering of neutrons is included. This figure shows that source
 119 neutrons with different energies produce different responses, that is different measured
 120 spectra in the liquid scintillators. This differentiation is the basis for inferring the en-
 121 ergy spectrum of the neutrons incident on the liquid scintillators, from the measured
 122 spectrum in the scintillators.

123 The last set of curves in Fig. 6 shows the probability density functions for the
 124 electron-equivalent energies deposited by the neutrons in the liquid scintillators. To
 125 produce these distributions, each distribution in Fig. 5 was normalized, and each bin of
 126 the normalized distribution was divided by the bin width. Integrated over the energy
 range, each cumulative density function thus produced is equal to 1.

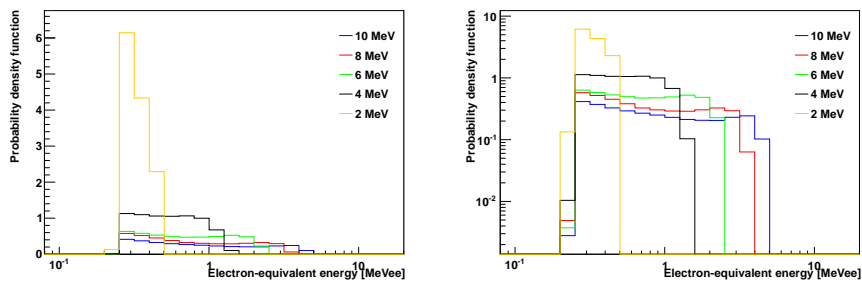


Figure 6: Probability density functions of the energy distributions measured by the liquid scintillators as predicted by MCNPX. The different colors refer to different initial neutron energies. (For interpretation of the references to color in this figure caption, the reader is referred to the web version of this paper.)

127

128 *3.1. First method to determine multiple scattering fractions*

For these 19 initial neutron energies between 1 MeV and 10 MeV, we computed the fractions of single source neutrons registering counts in two and three liquid scintillators. The simulations were such that (a) the system does not multiply neutrons, so that both M and qM are equal to 1, and (b) neutrons are emitted one at a time, so that both D_{2s} and D_{3s} are zero. In these conditions, many terms disappear in the system of equations (13), and we can write the following equations that apply to non-multiplying sources emitting single neutrons at a time:

$$\begin{cases} \bar{C}(T) = (1 + f_2 + 2f_3) R_1^* T \\ Y_2(T) = (f_2 + 3f_3) R_1^* T \\ Y_3(T) = f_3 R_1^* T \end{cases} \quad (15)$$

129 where $Y_2(T)$ and $Y_3(T)$ are equal to $Y_{2F}(T) \bar{C}(T)$ and $Y_{3F}(T) \bar{C}(T)$, respectively. This
 130 system of 3 equations has 3 unknowns. The fractions of doubles f_2 and triples f_3
 131 as well as the hypothetical count rate R_1^* can be determined by taking the slopes of
 132 Eqs. (15).

133 Let's look at the quantities $\bar{C}(T)$, $Y_2(T)$, and $Y_3(T)$ calculated from a MCNPX Monte
 134 Carlo simulation of a weak 8 MeV-neutron source in the middle of the 77 liquid scintillator
 135 array (depicted in Fig. 1). Using LLNL's customized version [9] of MCNPX, neutrons
 136 are transported from spontaneous fission to the liquid scintillators, where their
 137 times of detection are recorded. Splitting the sequence of time tags into segments as
 138 explained in Sec. 2, we build count distributions $B_n(T)$. In the top left quadrant of
 139 Fig. 7, the blue points are $B_n(T)$ for $T=512$ ns. In the other 3 quadrants, $\bar{C}(T)$, $Y_2(T)$
 140 and $Y_3(T)$ were calculated from this 512 ns count distribution, as well as for 5 other
 141 Monte Carlo generated count distributions for time gate durations in geometric pro-
 142 gression between 16 and 512 ns. The green curves are analytical (see Eqs. (16) below)
 143 fits to the blue Monte Carlo data points. The slopes of $\bar{C}(T)$ in the top right quadrant,
 144 of $Y_2(T)$ and $Y_3(T)$ in the bottom quadrants of Fig. 7 are the factors of T in Eqs. (15)
 145 and (16).

Given the size of the liquid scintillators (10-cm-diameter), and the speed of ~ 1.5 cm/ns
 of 1 MeV neutrons, it would take a neutron at least 7 ns to register a count in a scintilla-
 tor, register a count in a second scintillator and travel 10 cm to get to a third scintillator.
 Even for 4 MeV neutrons traveling twice as fast, it would take 3.5 ns for them to reg-
 ister counts in 3 different scintillators. From this follows that the slope of $Y_3(T)$ is
 not quite as steep when T is close to 0. The same applies to $Y_2(T)$. Because of this
 unmodeled latency — even though short — $Y_2(T)$ and $Y_3(T)$ in Fig. 7 are not exactly
 fit by the linear functions (15), but by affine versions thereof with identical slopes:

$$\begin{cases} \bar{C}(T) = (1 + f_2 + 2f_3) R_1^* T \\ Y_2(T) = (f_2 + 3f_3) R_1^* (T - T_2^0) \\ Y_3(T) = f_3 R_1^* (T - T_3^0) \end{cases} \quad (16)$$

146 The values of f_2 , f_3 and R_1^* can be determined by solving the system of equations (16).
 147 Interestingly, T_2^0 and T_3^0 give orders of magnitude for the times it takes for neutrons

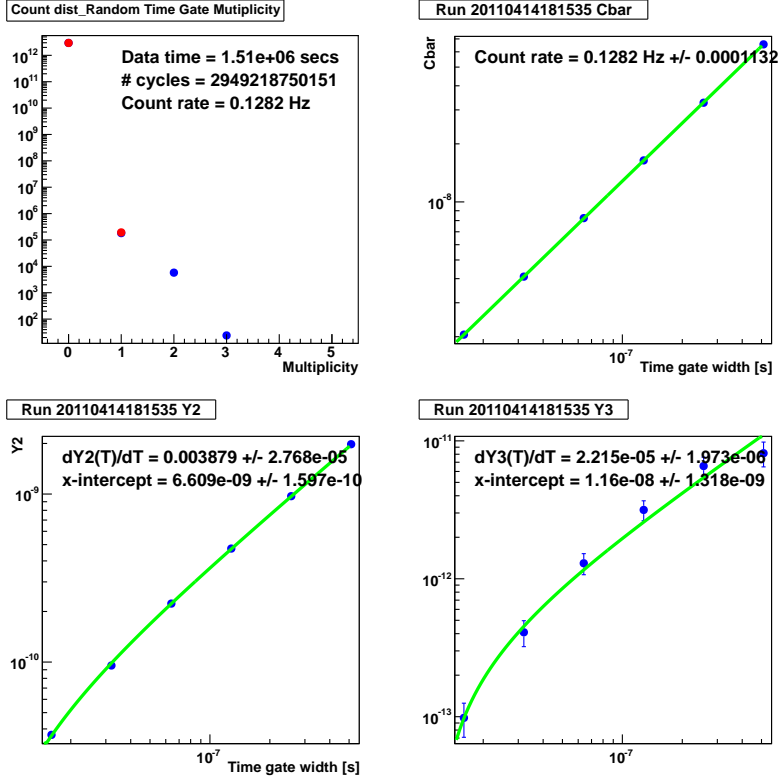


Figure 7: Count distribution $B_n(T=512 \text{ ns})$, $\bar{C}(T)$, $Y_2(T)$ and $Y_3(T)$ as a function of time gate width T , for T ranging between 16 ns and 512 ns. $\bar{C}(T)$, $Y_2(T)$ and $Y_3(T)$ are fit using Eqs. (16). The data are from a MCNPX simulation of 8 MeV neutrons in the middle of the liquid scintillator array shown in Fig. 1. Blue is Monte Carlo data, green is theoretical fit. (For interpretation of the references to color in this figure caption, the reader is referred to the web version of this paper.)

148 to register 2 and 3 liquid scintillator counts, respectively. Fig. 7 reveals that 8-MeV
 149 neutrons take in average ~ 6.6 ns to scatter from one liquid scintillator to another one,
 150 while they take in average ~ 12 ns to scatter from one liquid scintillator to two other
 151 ones, consecutively. The reason why triple-scattering does not take twice as long as
 152 double-scattering can be explained. When a neutron scatters and records counts in 2
 153 scintillators, the energy of the neutron between the first and second scintillators can be
 154 as low as 1.2 MeV (threshold for detection of fast neutrons). For a neutron to scatter
 155 and record counts in 3 scintillators, the energy of the neutron between the first and
 156 second scintillators has to be at least 2.4 MeV. Otherwise, the fast neutron — which
 157 needs to deposit at least 1.2 MeV in the second scintillator to be counted, and would
 158 thus be left with at the most 1.2 MeV after the second scintillator — would not have
 159 the required 1.2 MeV of energy to record a count in a third scintillator. Therefore, for
 160 three counts to be recorded, the speed of the neutron between the first and the second
 161 scintillator has to be at least 1.4 times greater than the speed of a neutron recording

162 only two counts. Thus, we can conclude that the time it takes for a neutron to record 3
 163 counts in a liquid scintillator array will be less than twice the time it takes for a neutron
 164 to record 2 counts in the same liquid scintillator array. We should point out that the
 165 quantities T_2^0 and T_3^0 in Eqs. 16 are small, and that their introduction negligibly affects
 166 the slopes. Therefore, Eqs. 15 will be used from now on.

167 The fractions f_2 and f_3 of neutrons scattering multiple times and registering two
 168 and three counts in the liquid scintillator array are shown in Fig. 8 for a range of source
 neutron energies. The fraction of neutrons scattering multiple times and registering

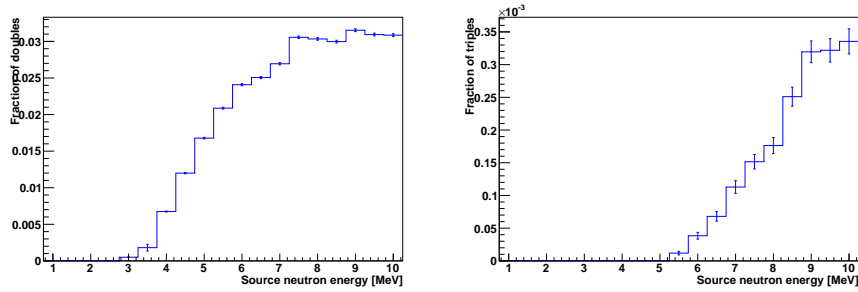


Figure 8: Fractions f_2 and f_3 of detected neutrons registering two and three counts in the liquid scintillator array, as a function of the source neutron energies.

169 four counts in the liquid scintillator array is shown in Fig. 3. For all simulations, the
 170 threshold for detection in the liquid scintillators was set to 250 keVee. This value is
 171 not arbitrary, and corresponds to the energy above which pulse shape discrimination
 172 for liquid scintillators works well. Below 250 keVee, neutrons and photons cannot be
 173 distinguished as reliably.
 174

175 Because the count rate is artificially inflated by the neutrons registering multiple
 176 counts in the liquid scintillator array, the hypothetical count rate differs from the mea-
 177 sured count rate as shown in Fig. 9. This figure shows the hypothetical count rate R_1^*
 178 and measured count rates R_1 as a function of the source neutron energies. Note that
 179 the 3 plotted count rates are exactly matched up to 3 MeV, and are thus hidden behind
 180 each other. Furthermore, the “Measured count rate R_1 ” and “Count rate R_1 determined
 181 by method 2” are indistinguishable all the way to 10 MeV.

182 The right graph in Fig. 9 shows the absolute neutron detection efficiency of the
 183 liquid scintillator array. The detection efficiency is maximum for neutron energies
 184 around 3.5 MeV and 4 MeV, and decreases steadily as the neutron energy increases.
 185 Fast neutrons 1 MeV and lower are undetectable. This is because 1 MeV neutrons
 186 produce quenched energies of the order of 250 keVee, which is our detection threshold,
 187 as explained above.

188 The fractions f_2 and f_3 of neutrons scattering multiple times are listed in table 1
 189 for different mono-energetic neutron sources.

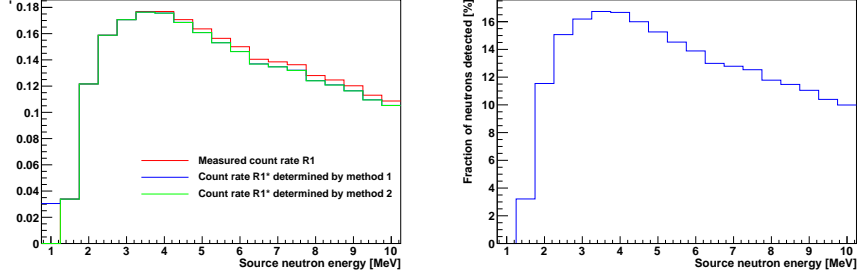


Figure 9: Comparison between the measured count rate R_1 , the count rate R_1^* predicted by the system of equations (13) and the count rate predicted by the second method, as a function of the different initial neutron energies. Neutron detection efficiency of liquid scintillator array, as a function of neutron energy.

Table 1: Fractions f_2 and f_3 of neutrons double- and triple-scattering between liquid scintillators in the liquid scintillator array shown in Fig. 1, for mono-energetic and fissile neutrons. The liquid scintillator energy threshold is 250 keVee.

Neutron source	f_2 [%]	f_3 [%]
1.5 MeV	0.000e+00	0.000e+00
2.0 MeV	0.000e+00	0.000e+00
2.5 MeV	0.000e+00	0.000e+00
3.0 MeV	5.008e-02	0.000e+00
3.5 MeV	1.808e-01	0.000e+00
4.0 MeV	6.746e-01	0.000e+00
4.5 MeV	1.199e+00	0.000e+00
5.0 MeV	1.678e+00	0.000e+00
5.5 MeV	2.088e+00	1.188e-03
6.0 MeV	2.408e+00	3.843e-03
6.5 MeV	2.506e+00	6.802e-03
7.0 MeV	2.695e+00	1.129e-02
7.5 MeV	3.056e+00	1.516e-02
8.0 MeV	3.034e+00	1.763e-02
8.5 MeV	2.998e+00	2.510e-02
9.0 MeV	3.153e+00	3.195e-02
9.5 MeV	3.094e+00	3.219e-02
10.0 MeV	3.086e+00	3.355e-02
^{238}U	2.786e-01	0.000e+00
^{240}Pu	3.875e-01	3.407e-04
^{252}Cf	4.245e-01	9.739e-04
2.2 MeV (Fig. 12)	0.000e+00	0.000e+00
4.4 MeV (Fig. 10)	1.113e+00	0.000e+00

Neutron source	f_2 [%]	f_3 [%]
7.24 MeV (Fig. 11)	2.680e+00	1.307e-02

190 One should point out that the multiple scattering fractions f_2 and f_3 greatly depend
191 on the geometry of the liquid scintillator array and on the energy threshold of the liquid
192 scintillators. The values in table 1 are only valid for the geometry shown in Fig. 1 and
193 for a liquid scintillator energy threshold of 250 keVee.

194 3.2. Second method to determine multiple scattering fractions

195 To make sure the analysis using the system of equations (13) was derived prop-
196 erly, we derived the numbers of multiple scatterings not from a statistical perspective,
197 but from an alternative second method. This can be done simply using the procedure
198 described here: each fast neutron count registered by the liquid scintillators triggers
199 a time window of duration T and one counts how many fast neutrons are within that
200 window. If there is one fast neutron in the window, then this count along with the one
201 that triggered the window will be consolidated into a single double scattering count. If
202 there were two fast neutrons in the window, then these 2 counts along with the trigger
203 count will be consolidated into a single triple scattering count. The empty windows are
204 considered single scattering events, because they only contain the trigger event. The
205 fractions of doubles and triples are quasi-identical to the ones shown in Fig. 8, the count
206 rates do not differ much either, as shown by the “method 2” line in Fig. 9. These two
207 ways of producing the same data gives us confidence that the models used to predict
208 the unknowns R_1^* , f_2 and f_3 are correct.

209 The advantage of the method laid out in Sec. 3.1 is on the experimental side. When
measuring the double and triple-scattering fractions of neutrons experimentally, the
method does not require a neutron source emitting single neutrons (such as AmBe or
AmLi). Any non-multiplying ($M=1$) spontaneous fission source (such as ^{252}Cf) of
known source intensity $\bar{v}_{\text{sp}}F_s$ can be used to measure the multiple scattering fractions
using the system of equations derived from Eqs. (13):

$$\begin{cases} R_1 = (1 + f_2 + 2f_3) \epsilon \bar{v}_{\text{sp}} F_s \\ R_{2F} = \frac{f_2 + 3f_3}{1 + f_2 + 2f_3} + (1 + f_2 + 2f_3) \epsilon D_{2s} \\ R_{3F} = \frac{f_3}{1 + f_2 + 2f_3} + 2(f_2 + 3f_3) \epsilon D_{2s} + (1 + f_2 + 2f_3)^2 \epsilon^2 D_{3s} \end{cases} \quad (17)$$

210 as long as the source is not contaminated by (α, n) neutrons⁸. Using a time-tagged
211 ^{252}Cf source for instance, we can experimentally measure R_1 , R_{2F} and R_{3F} , and solve
212 the system of equations (17) for ϵ , f_2 and f_3 . This is an important advantage over
213 method 2, which intrinsically does not account for the fact that spontaneous fissions
214 emit multiple neutrons simultaneously.

⁸This is a permissible approximation for a pure, non-sealed and unshielded source.

If the intensity of the non-multiplying spontaneous fission source is not known, we can use the equation for R_{4F} as well:

$$R_{4F} = \left(\frac{(f_2 + 3f_3)^2}{1 + f_2 + 2f_3} + 2f_3 \right) \varepsilon D_{2s} + 3(1 + f_2 + 2f_3)(f_2 + 3f_3) \varepsilon^2 D_{3s} + (1 + f_2 + 2f_3)^3 \varepsilon^3 D_{4s} \quad (18)$$

215 4. Input spectrum reconstruction

216 Before trying to determine the factors f_2 and f_3 , we will see if we can reconstruct
 217 the spectra of 3 different mono-energetic neutron sources, based on the set of measured
 218 spectra shown in Fig. 5. We use the subscript E_i to distinguish each one of the basis
 219 functions $g_{E_i}(E_d)$ shown in Fig. 5. The subscript E_i denotes the initial source neutron
 220 energy, from 1 MeV up to 10 MeV, in increments of 0.5 MeV. Given a measured spec-
 221 trum $\tilde{g}(E_d)$, the goal for the reconstruction is to find the set of weights w_{E_i} for which
 222 the difference between $\tilde{g}(E_d)$ and the reconstructed liquid scintillator energy spectrum
 223 is minimized. Each weight w_{E_i} is physically to be interpreted as the intensity of the
 224 neutron source in the energy bin around E_i .⁹

Let's call $g^r(E_d)$ the reconstructed energy deposition spectrum. $g^r(E_d)$ is defined as

$$g^r(E_d) = \sum_{i=1}^{19} w_{E_i} g_{E_i}(E_d) \quad (19)$$

The optimal set of weights w_{E_i} will be such as to minimize

$$g^r(E_d) - \tilde{g}(E_d) \quad (20)$$

In order to minimize Eq. (20), we use χ^2 minimization algorithm implemented by Minuit in ROOT [10]. Based on this optimization, an estimate of the source neutron spectrum will be given by the energies E_i weighed by the weights w_{E_i} . For mono-energetic neutron sources, the estimated average source neutron energy E^{est} will be given by the w_{E_i} weighed average of the E_i .

$$E^{\text{est}} = \sum_{i=1}^{19} w_{E_i} E_i \quad (21)$$

Based on the solution set for the weights w_{E_i} , we can estimate the spectrum of electron-equivalent energies deposited by the neutrons in the liquid scintillator using

$$g^{\text{est}}(E_d) = \sum_{i=1}^{19} w_{E_i} g_{E_i}(E_d) \quad (22)$$

⁹If the distribution $\tilde{g}(E_d)$ is normalized, the weights w_{E_i} will be the relative intensities of the different neutron sources of energy E_i .

225 *4.1. Reconstruction of mono-energetic neutron sources*

226 We ran a few Monte Carlo simulations similar to the ones in Sec. 3, but with en-
 227 ergies not among the E_i for which we have basis functions. The first simulation was
 228 a mono-energetic 4.4 MeV neutron source. The blue histogram in Fig. 10a shows the
 229 spectrum measured by the modeled liquid scintillators, along with the best reconstruction
 230 $g^{\text{est}}(E_d)$ in red. The reconstruction $g^{\text{est}}(E_d)$ is not perfect but nonetheless a very
 231 good approximation of $\tilde{g}(E_d)$. Fig. 10b shows the reconstruction of the neutron source
 spectrum, which is basically the set of weights w_{E_i} . Using Eq. (21), the reconstructed

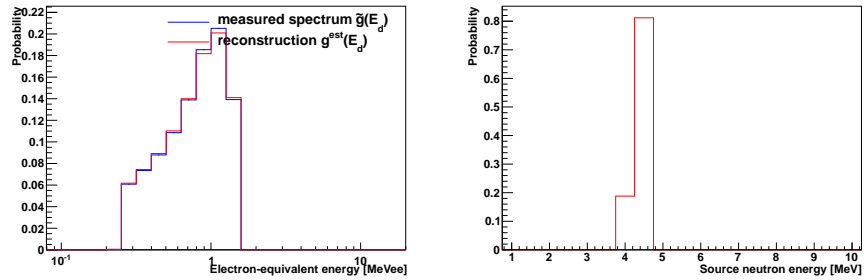


Figure 10: (a) Measured spectrum $\tilde{g}(E_d)$ (blue) and reconstructed spectrum $g^{\text{est}}(E_d)$ (red) of energies deposited by the neutrons, evaluated from Eq. (22). (b) Reconstruction of the source neutron energy spectrum. The estimated average source neutron energy is 4.406 MeV. The data is from a MCNPX simulation of a mono-energetic 4.4 MeV neutron source. (For interpretation of the references to color in this figure caption, the reader is referred to the web version of this paper.)

232 average neutron source energy was estimated to be 4.406 MeV.

233 The second and third simulations are mono-energetic 7.24 MeV and 2.2 MeV neu-
 234 tron source in the middle of the same liquid scintillator array. The blue histograms in

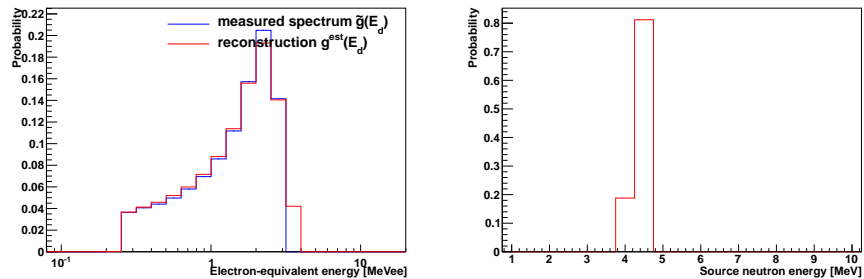


Figure 11: (a) Measured spectrum $\tilde{g}(E_d)$ (blue) and reconstructed spectrum $g^{\text{est}}(E_d)$ (red) of energies deposited by the neutrons, evaluated from Eq. (22). (b) Reconstruction of the source neutron energy spectrum. The estimated average source neutron energy is 7.51 MeV. The data is from a MCNPX simulation of a mono-energetic 7.24 MeV neutron source. (For interpretation of the references to color in this figure caption, the reader is referred to the web version of this paper.)

235 Figs. 11a and 12a show the spectra $\tilde{g}(E_d)$ measured by the liquid scintillators, along
 236

237 with the best reconstructions $g^{\text{est}}(E_d)$ in red. Figs. 11b and 12b show the reconstruc-
 238 tions of the neutron source spectra. The average energies determined from the reconstruc-
 239 tions were 7.51 MeV and 2.22 MeV. From these few data points, we observe that
 240 the predictions of the source neutron energies are good, but not perfect. Fig. 11b in-
 241 deed shows that there is a somewhat unexpected secondary peak at 8.5 MeV, while we
 242 would have expected a secondary peak at 7.5 MeV.

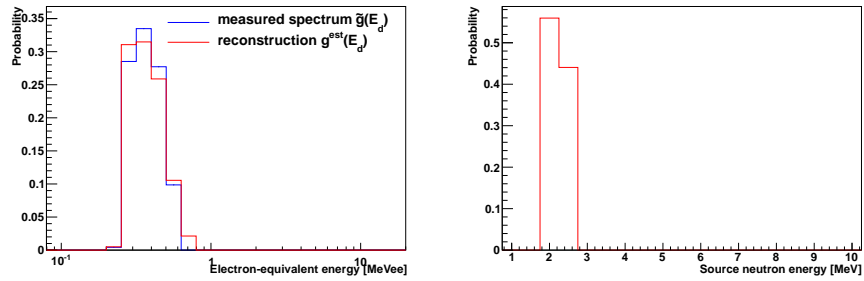


Figure 12: (a) Measured spectrum $\bar{g}(E_d)$ (blue) and reconstructed spectrum $g^{\text{est}}(E_d)$ (red) of energies deposited by the neutrons, evaluated from Eq. (22). (b) Reconstruction of the source neutron energy spectrum. The estimated average source neutron energy is 2.22 MeV. The data is from a MCNPX simulation of a monoenergetic 2.2 MeV neutron source. (For interpretation of the references to color in this figure caption, the reader is referred to the web version of this paper.)

243 **4.2. Reconstruction of spontaneous fission sources**

244 The next test is to see whether the reconstruction algorithm could predict the neu-
 245 tron spectrum emitted by spontaneous fission sources. Of course, the caveat here is
 246 one should not expect to predict the source neutron spectrum under approximately
 247 1.25 MeV, since liquid scintillators cannot reliably distinguish neutrons from photons
 248 neutrons below that energy.

249 We performed a simulation of a ^{252}Cf source. Fig. 13a shows the measured spec-
 250 trum $\tilde{g}(E_d)$ in blue and the reconstructed spectrum $g^{\text{est}}(E_d)$ in red. The reconstruction
 251 of the source neutron spectrum is shown in Fig. 13b. As expected, the source neutron
 252 spectrum reconstruction fails below 1.5 MeV for the reasons mentioned above. The
 253 estimated average source neutron energy is 3.05 MeV, but this value cannot be com-
 254 pared to the true average energy of ^{252}Cf spontaneous fission neutrons, because it is
 255 computed over the truncated energy distribution shown in Fig. 13b.

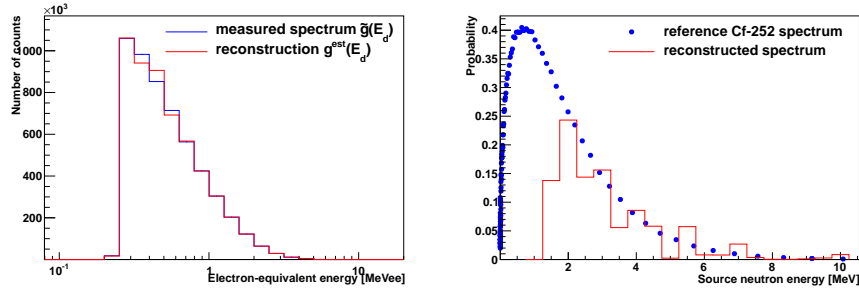


Figure 13: (a) Measured spectrum $\tilde{g}(E_d)$ (blue) and reconstructed spectrum $g^{\text{est}}(E_d)$ (red) of electron-equivalent energies deposited by the neutrons, evaluated from Eq. (22). (b) Reconstruction of the source neutron energy spectrum (red), along with the true ^{252}Cf spectrum (blue) from Ref. [11]. The data is from a MCNPX simulation of a ^{252}Cf source. (For interpretation of the references to color in this figure caption, the reader is referred to the web version of this paper.)

256 **5. Prediction of multiple scattering correction**

To predict multiple scattering corrections, we first measure the spectrum of fast neutrons in the liquid scintillators. Then the basis functions given in Fig. 4 are used to reconstruct the measured spectrum by minimizing Eq. 20. This minimization process will produce the weights w_{E_i} in $g^f(E_d)$ (see Eq. 19). Knowing these weights, we can estimate the fraction of double scattering f_2 and triple scattering f_3 by weighing the fractions $f_2(E_i)$ and $f_3(E_i)$ at different source energies E_i by w_{E_i} :

$$f_2 = \sum_{i=1}^{19} w_{E_i} f_2(E_i) \quad (23)$$

$$f_3 = \sum_{i=1}^{19} w_{E_i} f_3(E_i) \quad (24)$$

257 The functions $f_2(E_i)$ and $f_3(E_i)$ are the curves shown in Fig. 8. Values for f_2 and f_3
 258 are also given in Table 1. For the 3 mono-energetic neutron sources of section 4.1, and
 259 the ^{252}Cf source of section 4.2, the estimated fractions f_2 and f_3 are given in table 1.

260 6. Application to NMC: mass correction using multiple scattering correction

261 A Monte Carlo simulation was run to see if the intensity of a ^{252}Cf source could be
 262 more accurately determined using the multiple scattering correction factors f_2 and f_3 .
 263 For this simulation, we used the same geometry as for the previous cases. The input
 264 source intensity was 39,761 neutrons/s. The count distribution B_n , along with \bar{C} , Y_{2F}
 265 and Y_{3F} are shown in Fig. 14.

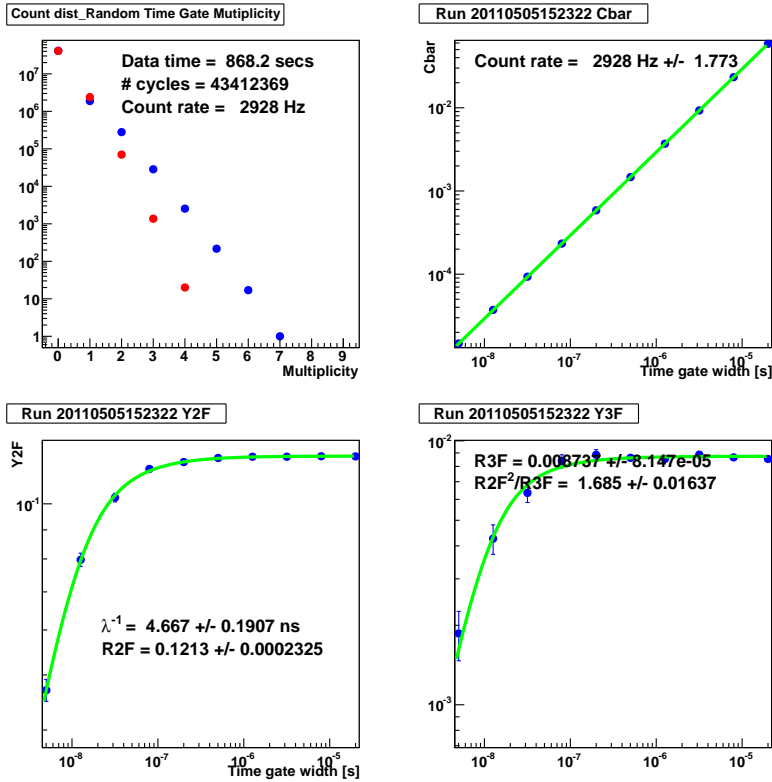


Figure 14: Count distribution $B_n(T = 20 \mu s)$ and $\bar{C}(T)$, $Y_2(T)$ and $Y_3(T)$ as a function of time gate width T . λ^{-1} denotes α^{-1} . $\bar{C}(T)$, $Y_2(T)$ and $Y_3(T)$ are fit using Eqs. (1), (5) and (7), with A set to 0. The data are from an MCNPX simulation of a ^{252}Cf source in the middle of the liquid scintillator array shown in Fig. 1.

If we assume a multiplication¹⁰ M of 1 and an α -ratio A of 0, the first 2 equations

¹⁰According to the MCNPX output, the multiplication is about 1.0002.

of the system of equations (12) reduce to

$$\begin{cases} R_1 = \varepsilon \bar{v}_{\text{sp}} F_s \\ R_{2F} = \varepsilon D_{2s} \end{cases} \quad (25)$$

266 which has two unknowns F_s and ε . This system of two equations contains enough
 267 information to solve for the efficiency ε and the source intensity $\bar{v}_{\text{sp}} F_s$. We can thus
 268 solve for the mass of ^{252}Cf using this simulated data set. Knowing that D_{2s} is equal to
 269 1.595975 for ^{252}Cf , the detection efficiency ε is equal to 7.6% with a relative error of
 270 0.2% and the ^{252}Cf source intensity is $38,524 \pm 0.2\%$ neutrons/s. The source intensity is
 271 thus underestimated by 3.2% with the equations with no multiple scattering correction.

If we account for multiple scattering, we will use the following system of equations instead of Eqs. (25):

$$\begin{cases} R_1 = (1 + f_2 + 2f_3) \varepsilon \bar{v}_{\text{sp}} F_s \\ R_{2F} = \frac{f_2 + 3f_3}{1 + f_2 + 2f_3} + (1 + f_2 + 2f_3) \varepsilon D_{2s} \end{cases} \quad (26)$$

272 How do we determine the correction factors f_2 and f_3 ? Simply by measuring the
 273 neutron spectrum in the liquid scintillators. This measured spectrum is shown in blue
 274 in Fig. 13a. In red, the reconstruction $g^{\text{est}}(E_d)$ generates the weights w_{E_i} that we need
 275 to calculate f_2 and f_3 (using Eqs. 23 and 24). The corrections f_2 and f_3 for ^{252}Cf
 276 were already calculated in Sec. 5 and are in Table 1. Using these corrections, the
 277 source intensity now becomes 39,925 neutrons/s and the efficiency 7.3% with a relative
 278 error of 0.2%. With the multiple scattering correction, the source intensity is within 2
 279 standard deviations from the true value, which is a significant improvement over the
 280 estimate not using the multiple scattering correction.

281 We verified that Eqs. 26 also hold for mono-energetic random (i.e. uncorrelated)
 282 neutron sources emitting single neutrons at a time. In this case, we showed that the
 283 measured value of R_{2F} was equal to $\frac{f_2 + 3f_3}{1 + f_2 + 2f_3}$, which is consistent with an expected D_{2s}
 284 of 0. Of course, it is impossible to determine the detection efficiency ε , nor the mass
 285 of such sources in this case.

286 We should emphasize that the authors did not expect perfect reconstruction of the
 287 source intensity. The reasons are multiple: (a) we have seen in Sec. 4.2 that the method
 288 does not reconstruct neutron source spectra perfectly, which leads to an error in the
 289 estimation of the multiple scattering fractions. In that respect, using a larger number
 290 of mono-energetic neutron beams with intermediate energies might help. (b) The point
 291 model theory due to Feynman [2] on which this work is based, makes several assump-
 292 tions. One of them is that the neutron detection efficiency ε does not depend on the
 293 neutron energy. Whereas this is a reasonable assumption for ^3He tubes embedded in
 294 polyethylene, it is less so for liquid scintillators detecting fast neutrons, as shown in
 295 Fig. 9. Multiple scattering corrections are one of the corrections that is required to
 296 improve the reconstruction of the source mass, but it is only one of them.

297 7. Conclusion

298 With the help of theoretical expressions for the Feynman correlated moments of
 299 count distributions that account for multiple scatterings of neutrons, we showed that it

300 is possible to determine the fractions of neutrons scattering twice and thrice between
 301 liquid scintillators from the first 3 Feynman correlated moments of measured count
 302 distributions. These multiple scattering fractions can be determined for any neutron
 303 source, whether mono-energetic or not, and they strongly depend on the energy of the
 304 source neutrons.

305 For nuclear materials undergoing either spontaneous or induced fission, the same
 306 theoretical expressions for the Feynman correlated moments can be used in conjunction
 307 with the measured deposited energy spectrum to apply corrections to the estimates
 308 of the detection efficiency, the system multiplication, and the masses of the sources
 309 under measurement. A simple simulation using a californium source showed that the
 310 determination of the ^{252}Cf mass was improved using the multiple scattering correction.

311 Also, we were able to show that measuring the spectrum of fast neutrons depositing
 312 energy in the liquid scintillator array reveals spectral information about the neutron
 313 source.

314 Acknowledgments

315 This work was performed under the auspices of the U.S. Department of Energy by
 316 Lawrence Livermore National Laboratory under Contract DE-AC52-07NA27344.

317 Appendix A. Derivation of the Feynman correlated moment equations for neu- 318 trons scattering multiple times

319 In this appendix, we will derive the expressions for $\bar{C}(T)$, $Y_{2F}(T)$, $Y_{3F}(T)$ two
 320 different ways: using generating functions based on the work of Böhnell [12], and a
 321 second method in the line of Hage-Cifarelli [13].

322 Appendix A.1. Generating function

Let's consider the generating function for the $e_n(\varepsilon)$ distribution, which gives the
 probability of detecting n neutrons from a single fission chain. In the case when neu-
 trons never multiple scatter between liquid scintillators, the generating function for the
 $e_n(\varepsilon)$ distribution can be written as

$$h(d(y)) = \sum_{v=0}^{\infty} e_n(\varepsilon) y^n \quad (\text{A.1})$$

$$d(y) = (1 - \varepsilon) + \varepsilon y \quad (\text{A.2})$$

323 where $h(y)$ is the single neutron induced fission chain probability generating function
 324 defined by Eq. (12b) of Böhnell [12] and Eq. (34) of Prasad-Snyderman [4]. The gener-
 325 ating function parameter y in $h(y)$ must be replaced by detector probability generating
 326 function $d(y)$ through the compound process to account for detector efficiency ε .

When neutrons are allowed to multiple scatter between liquid scintillators, the generating function parameter y in $h(y)$ must be replaced, through the compound process, by the following detector probability generating function $f(y)$:

$$f(y) = (1 - \varepsilon) + \varepsilon(1 - f_2 - f_3)y + \varepsilon f_2 y^2 + \varepsilon f_3 y^3 \quad (\text{A.3})$$

327 where the first term $(1 - \varepsilon)$ — which could also be written as $(1 - \varepsilon)y^0$ — is the prob-
 328 ability that a neutron is not detected; the second term (or more precisely the coefficient
 329 of y) $\varepsilon(1 - f_2 - f_3)$ is the probability that a neutron is detected by a single liquid scintill-
 330 ator; the third polynomial coefficient εf_2 is the probability that a neutron is detected
 331 by a liquid scintillator, scatters and is detected once and only once more by another
 332 liquid scintillator; and finally the last polynomial coefficient εf_3 is the probability that
 333 a neutron is detected thrice by 3 different liquid scintillators. The powers in y count the
 334 number of times a single neutron is detected by the array: 0, 1, 2 or 3 times.

The single neutron induced fission chain probability generating function which accounts for neutrons to multiple scatter between liquid scintillators becomes:

$$h(f(y)) = \sum_{v=0}^{\infty} e_n(\varepsilon) y^n \quad (\text{A.4})$$

Taking the first derivative of $h(f(y))$ with respect to y , and setting y to 1, we get

$$\begin{aligned} \left. \frac{\partial h}{\partial y} \right|_{y=1} &= h' \Big|_{y=1} f' \\ &= \varepsilon h' \Big|_{y=1} ((1 - f_2 - f_3) + 2f_2 + 3f_3) \\ &= \varepsilon h' \Big|_{y=1} (1 + f_2 + 2f_3) \\ &= R_1^* (1 + f_2 + 2f_3) \end{aligned} \quad (\text{A.5})$$

The second derivative leads to

$$\begin{aligned} \left. \frac{1}{2!} \frac{\partial^2 h}{\partial y^2} \right|_{y=1} &= \frac{1}{2!} \left[h'' \Big|_{y=1} f'^2 + h' \Big|_{y=1} f'' \right] \\ &= \frac{1}{2!} h'' \Big|_{y=1} [\varepsilon(1 - f_2 - f_3) + 2\varepsilon f_2 + 3\varepsilon f_3]^2 + h' \Big|_{y=1} \varepsilon(f_2 + 3f_3) \\ &= R_2^* (1 + f_2 + 2f_3)^2 + R_1^* (f_2 + 3f_3) \end{aligned} \quad (\text{A.6})$$

Similarly, the third derivative is written as

$$\begin{aligned} \left. \frac{1}{3!} \frac{\partial^3 h}{\partial y^3} \right|_{y=1} &= \frac{1}{3!} \left[h''' \Big|_{y=1} f'^3 + 3 h'' \Big|_{y=1} f' f'' + h' \Big|_{y=1} f''' \right] \\ &= \frac{1}{3!} h''' \Big|_{y=1} \varepsilon^3 (1 + f_2 + 2f_3)^3 + h'' \Big|_{y=1} \varepsilon^2 (1 + f_2 + 2f_3)(f_2 + 3f_3) + h' \Big|_{y=1} \varepsilon f_3 \\ &= (1 + f_2 + 2f_3)^3 R_3^* + 2(1 + f_2 + 2f_3)(f_2 + 3f_3) R_2^* + f_3 R_1^* \end{aligned} \quad (\text{A.7})$$

If needed, the fourth derivatives reads

$$\begin{aligned}
\frac{1}{4!} \frac{\partial^4 h}{\partial y^4} \Big|_{y=1} &= \frac{1}{4!} \left[h''''|_{y=1} f'^4 + 6 h''''|_{y=1} f'^2 f'' + 3 h''|_{y=1} f''^2 + 4 h''|_{y=1} f' f''' + h'|_{y=1} f'''' \right] \\
&= \frac{1}{4!} \left[h''''|_{y=1} \varepsilon^4 (1 + f_2 + 2f_3)^4 + 6 h''''|_{y=1} \varepsilon^3 (1 + f_2 + 2f_3)^2 (2f_2 + 6f_3) \right. \\
&\quad \left. + 3 h''|_{y=1} \varepsilon^2 (2f_2 + 6f_3)^2 + 24 h''|_{y=1} \varepsilon^2 (1 + f_2 + 2f_3) f_3 \right] \\
&= (1 + f_2 + 2f_3)^4 R_4^* + 3 (1 + f_2 + 2f_3)^2 (f_2 + 3f_3) R_3^* \\
&\quad + (f_2 + 3f_3)^2 R_2^* + 2 (1 + f_2 + 2f_3) f_3 R_2^*
\end{aligned} \tag{A.8}$$

³³⁵ If needed, higher-order derivatives can be calculated trivially.

Dividing Eqs. (A.6), (A.7) and (A.8) by Eq. (A.5), we get the following equations for R_{2F} , R_{3F} and R_{4F} :

$$R_{2F} = \frac{f_2 + 3f_3}{1 + f_2 + 2f_3} + (1 + f_2 + 2f_3) R_{2F}^* \tag{A.9}$$

$$R_{3F} = \frac{f_3}{1 + f_2 + 2f_3} + 2(f_2 + 3f_3) R_{2F}^* + (1 + f_2 + 2f_3)^2 R_{3F}^* \tag{A.10}$$

$$R_{4F} = \left(\frac{(f_2 + 3f_3)^2}{1 + f_2 + 2f_3} + 2f_3 \right) R_{2F}^* + 3(1 + f_2 + 2f_3)(f_2 + 3f_3) R_{3F}^* + (1 + f_2 + 2f_3)^3 R_{4F}^* \tag{A.11}$$

³³⁶ *Appendix A.2. Combinatorial expansion*

An alternative way to get to the same result is by starting with $\Lambda_n(T)$, the probability to count n neutrons from the same fission chain in a random time gate of duration T . One can derive the expressions for $\bar{C}(T)$ starting from the equations¹¹ for the $\Lambda_n(T)$ including single neutrons registering multiple counts in different liquid scintillators in

¹¹See Eqs.(3), (54), (55) and Appendix B of Ref. [13], or Eq. A.20 in Ref. [14].

the limit of large time gate width T :

$$\begin{aligned}
\lim_{T \gg \alpha^{-1}} \frac{\Lambda_n(T)}{F_s T} &= \sum_{\nu=n}^{\infty} P_{\nu} \binom{\nu}{n} \varepsilon^n (1-\varepsilon)^{\nu-n} f_1^n \\
&+ \sum_{\nu=n-1}^{\infty} P_{\nu} \binom{\nu}{n-1} \varepsilon^{n-1} (1-\varepsilon)^{\nu-n+1} \binom{n-1}{1} f_1^{n-2} f_2 \\
&+ \sum_{\nu=n-2}^{\infty} P_{\nu} \binom{\nu}{n-2} \varepsilon^{n-2} (1-\varepsilon)^{\nu-n+2} \binom{n-2}{2} f_1^{n-4} f_2^2 \\
&+ \dots \\
&+ \sum_{\nu=n-2}^{\infty} P_{\nu} \binom{\nu}{n-2} \varepsilon^{n-2} (1-\varepsilon)^{\nu-n+2} \binom{n-2}{1} f_1^{n-3} f_3 \\
&+ \sum_{\nu=n-4}^{\infty} P_{\nu} \binom{\nu}{n-4} \varepsilon^{n-4} (1-\varepsilon)^{\nu-n+4} \binom{n-4}{2} f_1^{n-6} f_3^2 \\
&+ \dots \\
&+ \sum_{\nu=n-3}^{\infty} P_{\nu} \binom{\nu}{n-3} \varepsilon^{n-3} (1-\varepsilon)^{\nu-n+3} \frac{(n-3)!}{1!1!(n-5)!} f_1^{n-5} f_2 f_3 \\
&+ \sum_{\nu=n-4}^{\infty} P_{\nu} \binom{\nu}{n-4} \varepsilon^{n-4} (1-\varepsilon)^{\nu-n+4} \frac{(n-4)!}{2!1!(n-7)!} f_1^{n-7} f_2^2 f_3 \\
&+ \dots \\
&+ \sum_{\nu=n-5}^{\infty} P_{\nu} \binom{\nu}{n-5} \varepsilon^{n-5} (1-\varepsilon)^{\nu-n+5} \frac{(n-5)!}{1!2!(n-8)!} f_1^{n-8} f_2 f_3^2 \\
&+ \sum_{\nu=n-6}^{\infty} P_{\nu} \binom{\nu}{n-6} \varepsilon^{n-6} (1-\varepsilon)^{\nu-n+6} \frac{(n-6)!}{2!2!(n-10)!} f_1^{n-10} f_2^2 f_3^2 \\
&+ \dots
\end{aligned} \tag{A.12}$$

337 where f_2 and f_3 are the probabilities that a neutron detected in one liquid scintillator
338 scatters and registers one or two more counts in other liquid scintillators, respectively.
339 f_1 is the probability that a neutron detected in one liquid scintillator does not register
340 more counts in other liquid scintillators, so that the f distribution is normalized, $f_1 =$
341 $1 - f_2 - f_3$. If we were to account for higher order scattering events, we would have
342 $f_1 = 1 - \sum_{i=2}^{\infty} f_i$.

343 Here is how to interpret Eq. (A.12): the first term in the series is a summation
344 of probabilities to detect n neutrons from a single fission chain producing ν neutrons
345 where none of the ν neutrons registered multiple counts. Each one of the probabilities
346 in the sum is thus multiplied by f_1^n , the probability that none of the n neutrons detected
347 registered multiple counts. The second term in the series is a summation of proba-
348 bilities to detect n neutrons from a single fission chain producing ν neutrons, where
349 $n-2$ of the ν neutrons produced by the chain did not register multiple counts in liquid

350 scintillators, and one neutron from this fission chain registered two counts in differ-
 351 ent liquid scintillators. Each one of the probabilities in the sum is thus multiplied by
 352 f_1^{n-2} and f_2 : the probability that $n-2$ neutrons registered single detected events and
 353 the probability that one neutron was detected in two different scintillators. Because
 354 the neutron registering two counts can be any of the $n-1$ neutrons, we need to multi-
 355 ply these probabilities by the number of ways one can choose 1 neutron among $n-1$
 356 neutrons, i.e. $\binom{n-1}{1}$.

357 The first term in the second group of terms in Eq. (A.12) is a summation of proba-
 358 bilities to detect n neutrons from a single fission chain producing v neutrons, where
 359 $n-3$ of the v neutrons produced by the chain did not register multiple counts in liquid
 360 scintillators, and one neutron from this fission chain registered three counts in different
 361 liquid scintillators. Each one of the probabilities in the sum is thus multiplied by f_1^{n-3}
 362 and f_3 : the probability that $n-3$ neutrons registered single detected events and the
 363 probability that one neutron was detected in three different scintillators. Because the
 364 neutron registering three counts can be any of the $n-2$ neutrons, we need to multi-
 365 ply these probabilities by the number of ways one can choose 1 neutron among $n-2$
 366 neutrons, i.e. $\binom{n-2}{1}$.

If one denotes by $\Lambda_n^*(T)$ the expressions $\Lambda_n(T)$ when neutrons are not counted
 multiple times (i.e. with $f_{i>1} = 0$), we get

$$\lim_{T \gg \alpha^{-1}} \Lambda_n^*(T) = F_s T \sum_{v=n}^{\infty} P_v \binom{v}{n} \varepsilon^n (1-\varepsilon)^{v-n} \quad (\text{A.13})$$

One notices that each one of the terms in the series in Eq. (A.12) is a different order of
 $\Lambda_n^*(T)$ multiplied by a multinomial coefficient of the form

$$\frac{(\sum_{i=1}^{\infty} j_i)!}{\prod_{i=1}^{\infty} j_i!} \prod_{i=1}^{\infty} f_i^{j_i} \quad (\text{A.14})$$

367 The multinomial coefficients are counting the number of ways to distribute the different
 368 populations of neutrons (those registering one count, those registering two counts, etc.).

When there are only two kinds of multiple counts (e.g. f_1 and f_2), the multinomial
 reduces to a binomial coefficient

$$\binom{i+j}{i} f_m^i f_n^j \quad (\text{A.15})$$

Using the $\Lambda_n^*(T)$ notation, the first term of Eq. (A.12) becomes $f_1^n \Lambda_n^*$, the second term
 $\binom{n-1}{1} f_1^{n-2} f_2 \Lambda_{n-1}^*$, the third one $\binom{n-2}{2} f_1^{n-4} f_2^2 \Lambda_{n-2}^*$, etc. Eq. (A.12) can thus be rewrit-
 ten more compactly as

$$\lim_{T \gg \alpha^{-1}} \Lambda_n(T) = \sum_{j=0}^{j \leq n/3} \sum_{i=0}^{i \leq (n-3*j)/2} \frac{(n-2j-i)!}{i! j! (n-3j-2i)!} f_1^{n-3j-2i} f_2^i f_3^j \Lambda_{n-2j-i}^* \quad (\text{A.16})$$

The first few $\Lambda_n(T)$ are thus

$$\begin{aligned}
\lim_{T \gg \alpha^{-1}} \Lambda_1(T) &= \Lambda_1^* f_1 \\
\lim_{T \gg \alpha^{-1}} \Lambda_2(T) &= \Lambda_2^* f_1^2 + \Lambda_1^* f_2 \\
\lim_{T \gg \alpha^{-1}} \Lambda_3(T) &= \Lambda_3^* f_1^3 + \Lambda_2^* \binom{2}{1} f_1 f_2 + \Lambda_1^* f_3 \\
\lim_{T \gg \alpha^{-1}} \Lambda_4(T) &= \Lambda_4^* f_1^4 + \Lambda_3^* \binom{3}{1} f_1^2 f_2 + \Lambda_2^* f_2^2 + \Lambda_2^* \binom{2}{1} f_1 f_3
\end{aligned} \tag{A.17}$$

Using these expressions for $\Lambda_n(T)$, $\bar{C}(T)$ can be written as¹²

$$\begin{aligned}
\bar{C}(T) &= \sum_{i=1}^{\infty} \binom{i}{1} \Lambda_i \\
&= (1 + f_2 + 2f_3) \sum_{i=1}^{\infty} \binom{i}{1} \Lambda_i^* \\
&= (1 + f_2 + 2f_3) \bar{C}^*(T)
\end{aligned} \tag{A.18}$$

369 which means that the hypothetical $\bar{C}^*(T)$ ¹³ is increased by the factor $1 + f_2 + 2f_3$.
370 In the limiting case where f_2 is 1, that is, all neutrons register two counts in the liquid
371 scintillators, the measured count rate is twice the hypothetical count rate. In the limiting
372 case where f_3 is 1, where all neutrons register three counts in the liquid scintillators,
373 the measured count rate is thrice the hypothetical count rate. These two limiting cases
374 are consistent with our expectations.

Similarly, $Y_2(T)$ can be written as [4]

$$\begin{aligned}
Y_2(T) &= \sum_{i=2}^{\infty} \binom{i}{2} \Lambda_i \\
&= (f_2 + 3f_3) \bar{C}^*(T) + (1 + f_2 + 2f_3)^2 Y_2^*(T)
\end{aligned} \tag{A.19}$$

and $Y_3(T)$ as

$$\begin{aligned}
Y_3(T) &= \sum_{i=3}^{\infty} \binom{i}{3} \Lambda_i \\
&= f_3 \bar{C}^*(T) + 2(1 + f_2 + 2f_3)(f_2 + 3f_3) Y_2^*(T) + (1 + f_2 + 2f_3)^3 Y_3^*(T)
\end{aligned} \tag{A.20}$$

Dividing both expressions by $\bar{C}(T)$, we get

$$Y_{2F}(T) = \frac{f_2 + 3f_3}{1 + f_2 + 2f_3} + (1 + f_2 + 2f_3) Y_{2F}^*(T) \tag{A.21}$$

¹²Equation (115) for Y_1 in Ref. [4].

¹³Hypothetical number of counts which one would measure if individual neutrons could not be counted multiple times.

and

$$Y_{3F}(T) = \frac{f_3}{1 + f_2 + 2f_3} + 2(f_2 + 3f_3)Y_{2F}^*(T) + (1 + f_2 + 2f_3)^2 Y_{3F}^*(T) \quad (\text{A.22})$$

375 **Nomenclature**

T	=	time gate duration.
$B_n(T)$	=	number of times n neutrons were counted a random time gate of duration T .
$b_n(T)$	=	probability to get n counts in a random time gate of duration T .
p	=	probability that a neutron will induce fission in a nucleus on interaction.
q	=	probability that a neutron will not induce fission in a nucleus on interaction.
M	=	multiplication of the object.
qM	=	escape multiplication.
F_s	=	intensity of spontaneous fission source in units of spontaneous fissions per second.
A	=	α -ratio, the ratio of neutrons emitted by sources emitting single neutrons to neutrons emitted by sources emitting multiple neutrons simultaneously.
C_n & C	=	probability that a fission will emit n neutrons in induced fission & induced fission multiplicity distribution.
C_n^{sp} & C^{sp}	=	probability that a fission will emit n neutrons in spontaneous fission & spontaneous fission multiplicity distribution.
D_n	=	n^{th} combinatorial moment of induced fission multiplicity distribution.
D_n^{sp}	=	n^{th} combinatorial moment of spontaneous fission multiplicity distribution.
P_v	=	probability that the fission chain created n neutrons (excluding those internally absorbed to create subsequent fissions).
e_n	=	probability of detecting n neutrons from a single fission chain.
$\bar{C}(T)$	=	number of counts averaged over all time gates of duration T .
$Y_{2F}(T)$	=	the excess over unity of the variance to mean ratio of $b_n(T)$, or physically speaking the correlated pairs relative to the counts, sometimes referred to as the Feynman correlated moment.
$Y_{3F}(T)$	=	the skewness to mean ratio of $b_n(T)$, or physically speaking the correlated triples relative to the counts.
$Y_2(T)$	=	$Y_{2F}(T)$ multiplied by $\bar{C}(T)$.
$Y_3(T)$	=	$Y_{3F}(T)$ multiplied by $\bar{C}(T)$.
R_1	=	count rate measured by the detector.
R_{2F}	=	asymptote of $Y_{2F}(T)$.
R_{3F}	=	asymptote of $Y_{3F}(T)$.
f_1	=	probability of counting individual neutrons once.
f_2	=	probability of counting individual neutrons twice.
f_3	=	probability of counting individual neutrons thrice.

376

- 377 $h(y)$ = generating function for the e_n distribution.
- R_1^* = the hypothetical count rate which one would measure if individual neutrons could not be counted multiple times.
- $R_n^*(T)$ = the hypothetical value of $R_n = \frac{1}{n!} \frac{\partial^n h(y)}{\partial y^n}$ which one would obtain if individual neutrons could not be counted multiple times.
- E_d = electron-equivalent energy measured by liquid scintillators and deposited by fast neutrons.
- 378 $\tilde{g}(E_d)$ = measured liquid scintillator spectrum.
- $g_{E_i}(E_d)$ = probability that a source neutron of initial energy E_i will deposit an electron-equivalent energy within bin E_d . Basis functions for spectrum reconstruction.
- $g^r(E_d)$ = reconstructed liquid scintillator spectrum using basis functions $g_{E_i}(E_d)$.
- 379 Greek:
- ε = detection efficiency, or probability to detect a neutron.
- $\bar{\nu}$ = average number of neutrons produced in induced fission.
- $\bar{\nu}_{sp}$ = average number of neutrons produced in spontaneous fission.
- α = inverse fission chain evolution time scale.
- 380 $\Lambda_n()$ = probability to count n neutrons from the same fission chain in a random time gate of duration T .
- $\Lambda_n^*()$ = hypothetical probability to count n neutrons from the same fission chain in a random time gate of duration T , when individual neutrons are not counted multiple times.

- 381 [1] J. M. Verbeke, A. M. Glenn, G. J. Keefer, R. E. Wurtz, Multiple Scattering Cor-
382 rection for Liquid Scintillator Array: Experimental Measurements, LLNL-TR-
383 642085-DRAFT, Lawrence Livermore National Laboratory, 2013. [1](#)
- 384 [2] R.P. Feynman, F. De Hoffmann, R. Serber, Dispersion of the neutron emission in
385 U-235 fission, *Journal of Nuclear Energy*, **3**, (1-2, (August)), 1956, 64. [1](#), [2](#), [19](#)
- 386 [3] D.M. Cifarelli, W. Hage, Models for a Three-Parameter Analysis of Neutron Sig-
387 nal Correlation Measurements for Fissile Material Assay, *Nuclear Instruments*
388 *and Methods in Physics Research Section A* **251**, 1986, 550. [1](#), [2](#), [3](#)
- 389 [4] M.K. Prasad, N.J. Snyderman, Statistical Theory of Fission Chains and General-
390 ized Poisson Neutron Counting Distributions, *Nuclear Science and Engineering*
391 **172**, 300, 2012. [1](#), [2](#), [3](#), [4](#), [20](#), [25](#)
- 392 [5] S. Croft, A. Favalli, D.K. Hauck, D. Henzlova, P.A. Santi, Feynman variance-to-
393 mean in the context of passive neutron coincidence counting, *Nuclear Instruments*
394 *and Methods in Physics Research Section A* **686**, 2012, 136. [1](#), [2](#)
- 395 [6] J.M. Verbeke, G.F. Chapline, S.A. Sheets, Distinguishing Pu Metal
396 from Pu Oxide and Determining α -ratio using Fast Neutron Counting,
397 LLNL-JRNL-664381, Lawrence Livermore National Laboratory, 2015 (Nu-
398 clear Instruments and Methods in Physics Research Section A, in press,
399 <http://dx.doi.org/10.1016/j.nima.2015.01.088>). [2](#)
- 400 [7] D.B. Pelowitz, MCNPX User's Manual, Version 2.7.0, Los Alamos National Lab-
401 oratory, LA-CP-11-00438, 2012. [7](#)
- 402 [8] D.B. Pelowitz, J.W. Durkee, J.S. Elson, M.L. Fensin et al., MCNPX 2.7.0 Ex-
403 tensions, Los Alamos National Laboratory, Los Alamos, NM, LA-UR-11-02295,
404 2011. [7](#)
- 405 [9] J.M. Verbeke, Customized MCNPX to Generate "List-Mode" ^3He Neutron Cap-
406 tures and Scintillator Counts, LLNL-TM-671194, Lawrence Livermore National
407 Laboratory, 2015. [7](#), [9](#)
- 408 [10] R. Brun, F. Rademakers, ROOT - An Object Oriented Data Analysis Frame-
409 work, Proceedings AIHENP'96 Workshop, Lausanne, September 1996. See also
410 <http://root.cern.ch>. (Nuclear Instruments and Methods Physics Research Section
411 *A* **389**, 1997, 81). [14](#)
- 412 [11] Simulation of Neutron and Gamma Ray Emission from Fission and Photofission,
413 UCRL-AR-228518, Lawrence Livermore National Laboratory, 2010. [17](#)
- 414 [12] K. Böhnel, The effect of Multiplication on the Quantitative Determination of
415 Spontaneously Fissioning Isotopes by Neutron Correlation Analysis, *Nuclear Sci-*
416 *ence and Engineering* **90**, 1985, 75. [20](#)
- 417 [13] W. Hage, D.M. Cifarelli, Correlation Analysis with Neutron Count Distributions
418 in Randomly or Signal Triggered Time Intervals for Assay of Special Fissile Ma-
419 terials, *Nuclear Science and Engineering* **89**, 1985, 159-176. [20](#), [22](#)

- 420 [14] M. Prasad, N. Snyderman, J. Verbeke, R. Wurtz, Time Interval Distributions and
421 the Rossi Correlation Function, *Nuclear Science and Engineering* **174**, 2013, 1.
422 [22](#)